NASA CR-
141560

ASR 74-329

SPACE SHUTTLE
ORBIT MANEUVERING ENGINE
REUSABLE THRUST CHAMBER

(NAS9-12802)

TASK XIII

SUBSCALE HELIUM INGESTION AND TWO DIMENSIONAL HEATING TEST REPORT

ASR 74-329

SPACE SHUTTLE
ORBIT MANEUVERING ENGINE
REUSABLE THRUST CHAMBER

(NAS9-12802)

TASK XIII

SUBSCALE HELIUM INGESTION AND TWO DIMENSIONAL HEATING TEST REPORT

Prepared for

National Aeronautics and Space Administration
Johnson Spacecraft Center
Houston, Texas

Prepared by

R. D. Tobin
Advanced Projects

Approved by

R. P. Pauckert
SS/OME Principal Engineer
Advanced Programs

R. D. Paster
SS/OME Acting Program Manager
Advanced Programs

ROCKETDYNE DIVISION OF ROCKWELL INTERNATIONAL CORPORATION
6633 CANOGA AVENUE, CANOGA PARK, CA 91304

FOREWORD

This report, prepared in accordance with G.O. 07634 is submitted in accordance with Contract NAS9-12802, Exhibit A (Statement of Work), Task XIII (Subscale Helium Ingestion and Two Dimensional Heating).

ABSTRACT

Reported herein are descriptions of the test hardware, facility, procedures, and results of electrically heated tube, channel and panel tests conducted to determine effects of helium ingestion, two dimensional conduction, and plugged coolant channels on operating limits of convectively cooled chambers typical of Space Shuttle Orbit Maneuvering Engine designs.

Helium ingestion in froth form, was studied in tubular and rectangular single channel test sections. Plugged channel simulation was investigated in a three channel panel. Burn-out limits (transition to film boiling) were studied in both single channel and panel test sections to determine 2-D conduction effects as compared to tubular test results.

SUMMARY

A total of 103 electrically heated tube, channel, and panel tests were conducted to obtain data on the effects of geometry (2-D conduction), helium ingestion and plugged channels on MMH burnout limits. Eighty-five of the tests provided satisfactory data (the remainder were checkout, calibration, and tests wherein automatic cut occurred before stable conditions were achieved).

An initial test series (8 tests) with a symmetrically heated round CRES tube were conducted. These tests verified reproducibility of previous tube data to be used as a reference for the channel and panel tests. Nine tests were also conducted in the same tube with helium froth ingestion of varying amounts ranging from 5 to 30 percent by volume. These tests indicated a 15 to 20 percent reduction in MMH heat flux capability due to helium ingestion.

Thirty-seven tests were conducted with two different single channel geometries at two heated lengths simulating throat and injector end conditions. These tests indicated significant reduction in MMH burnout heat flux capability (based on 1-D values) at injector end conditions as predicted analytically. There was little effect of helium ingestion on maximum burnout heat flux levels in the channel test sections.

A total of 31 tests were performed with two 3-channel panels of markedly different geometry. Simple burn-out type tests agreed favorably with single channel data indicating the validity of the latter type test sections. Infinite helium bubble and plugged channel simulation tests showed that considerable cooling benefit is obtained from the adjacent MMH cooled channels.

INTRODUCTION

Under Task VII of the SS/OME Reusable Thrust Chamber Contract (NAS9-12802), electrically heated tube tests were conducted with MMH and 50-50 fuels to establish correlations for prediction of transition-to-film boiling (burnout) to be used in the prediction of local coolant safety factor in OME thrust chamber designs. These correlations were used to design two regeneratively cooled thrust chambers which were subsequently satisfactorily operated over a wide range of chamber pressures and mixture ratios simulating OME operating conditions.

Under Task IX of this contract certain adverse operating conditions were investigated to assess, in an economical manner, their possible impact on OME chamber operation. These adverse conditons included hot start simulation (as might occur during an ascent trajectory start with external heating from the SSME and SRB engines) and helium ingestion in either froth or discrete bubble form (should a bubble trap or surface tension device fail on the vehicle). In addition the effects of two-dimensional conduction on burn-out heat flux were investigated using asymmetrically heated rectangular passage test sections.

Task XIII of this contract (reported herein) essentially extended the effort initiated under Task IX in terms of helium ingestion and 2-D conduction effects. In addition, two asymmetrically heated panels composed of three rectangular channels each were evaluated to determine helium bubble, plugged channel, and 2-D conduction effects on operating limits.

Testing was conducted at the Thermal Laboratory of the B-1 Division of Rockwell International. The test program was performed in September 1974.

DISCUSSION

TEST FACILITY AND INSTRUMENTATION

Tests were conducted at the B-1 Division Thermal Laboratory, where previous OME heated tube test programs were conducted. The facility is shown schematically in Fig. 1 for tube and single channel tests and Fig. 2 for the three channel panel tests. Coolant flows from the pressurized tank through shutoff, throttle, and check valves into the test section. Flowrate is measured by turbine flowmeter(s) and calibrated orifice(s). A glass viewing section is installed downstream of the test section for visual and photographic observation of the flow with helium ingestion.

The test section consists of an electrically heated tube, channel, or panel section in a GN_2-purged box for safety (Fig. 3). Inlet and outlet pressures and temperatures of the coolant are measured. Wall temperatures are measured to indicate the onset of film boiling. Heating rates are controlled by the voltage applied to the ends of the test section via terminal bars. A back pressure regulator maintains the desired pressure at the end of the test section. GN_2 is used to purge the test section container and the flow system.

A GHe system is used for the helium ingestion tests. The system consists of a high-pressure GHe bottle, a regulator, a calibrated flow orifice, and a check valve. The helium system is connected, as shown in Fig. 1 or 2, for the helium froth tests. The mixer is a perforated tube sealed in a "T" (Fig. 4) which was located close to the test section to minimize agglomeration of the bubbles.

For the helium bubble tests, the mixer Tee is replaced with the bubble flow circuit shown in Fig. 1 or 2. Operation of this circuit is described under TEST PROCEDURES. Essentially, the system provides initial steady-state flow of MMH, followed by injection of a known quantity of helium at nearly constant

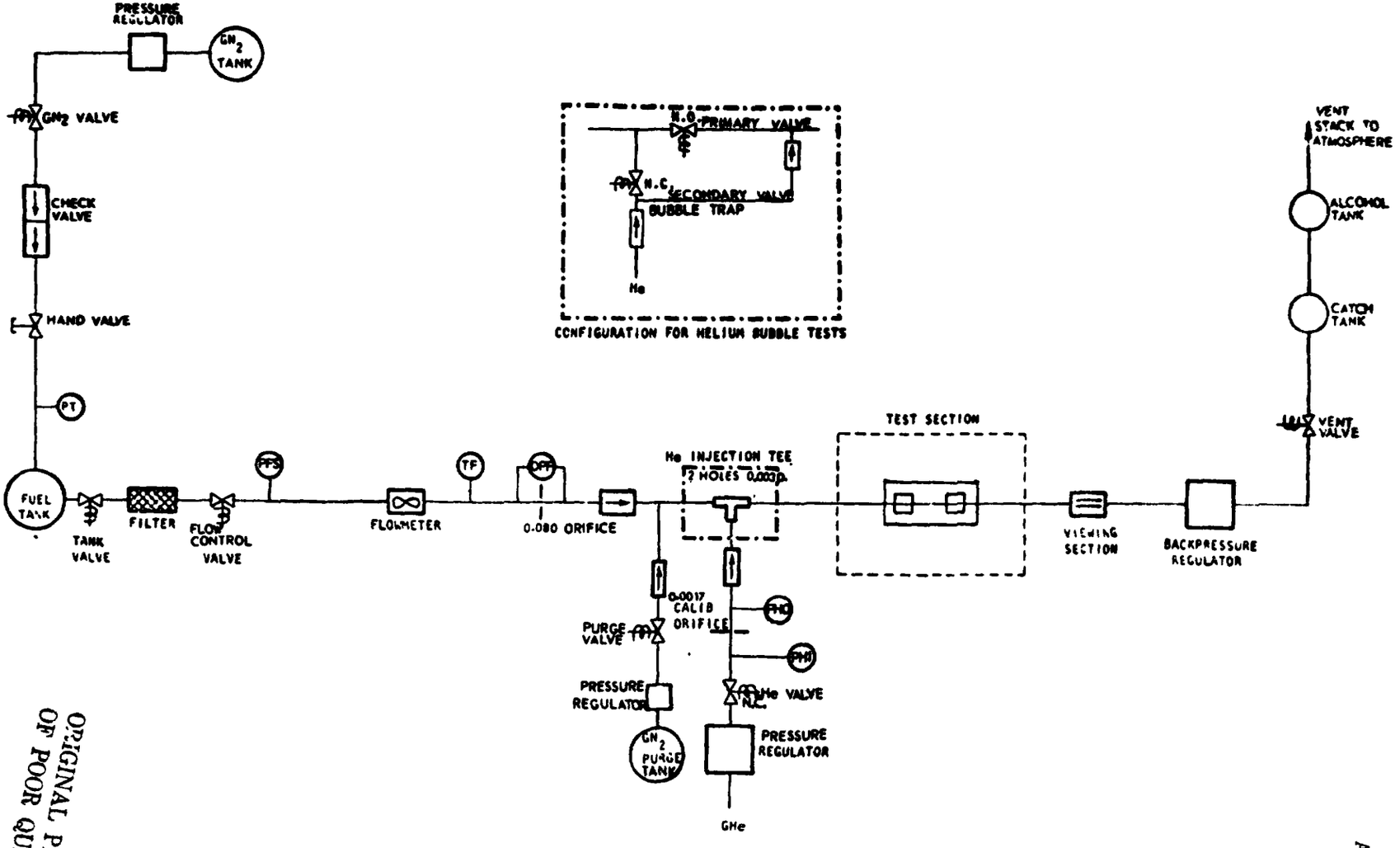

Figure 1. Facility Schematic for Heated Tube Tests

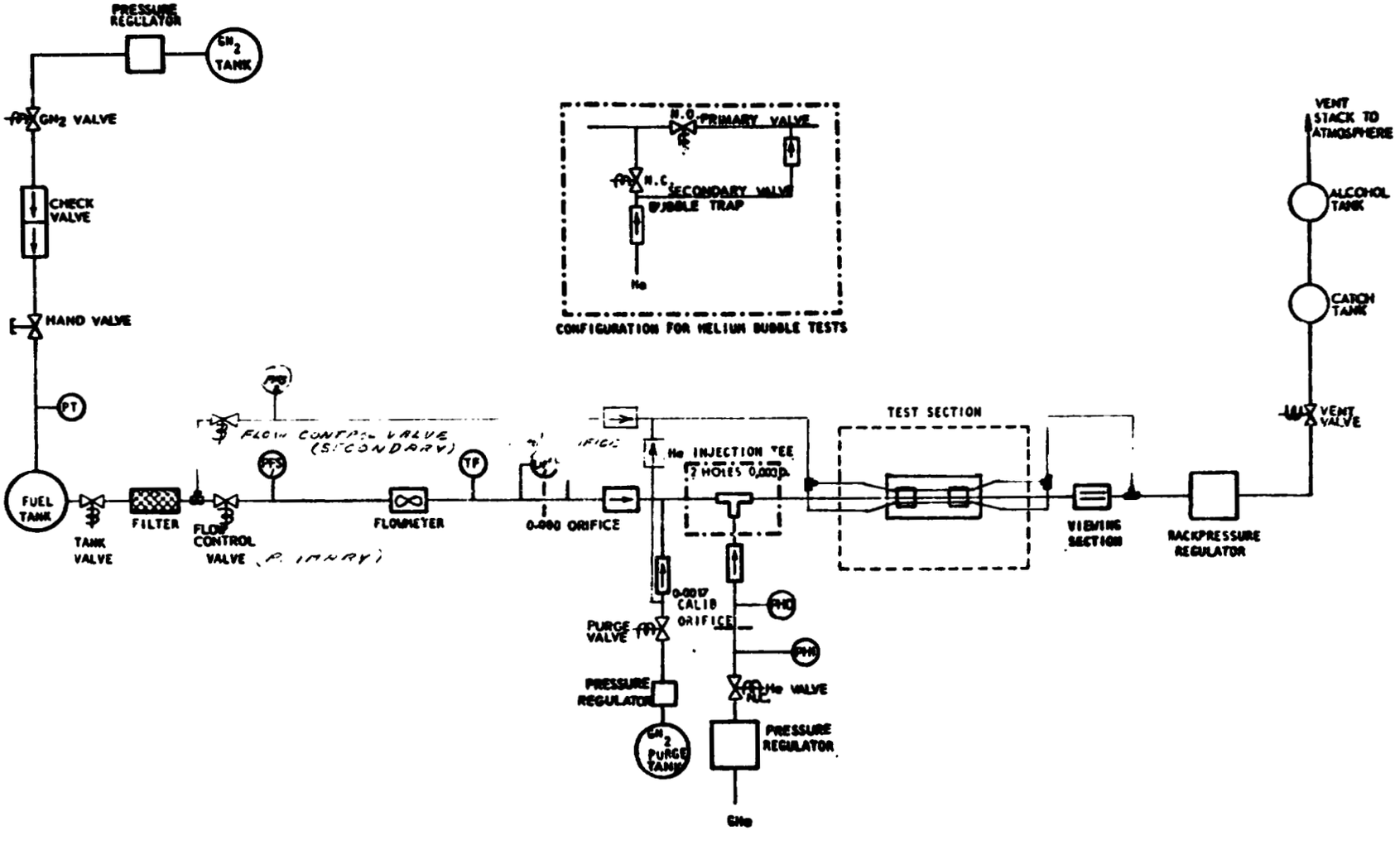

Figure 2. OME Three Passage Heated Tube Test Schematic

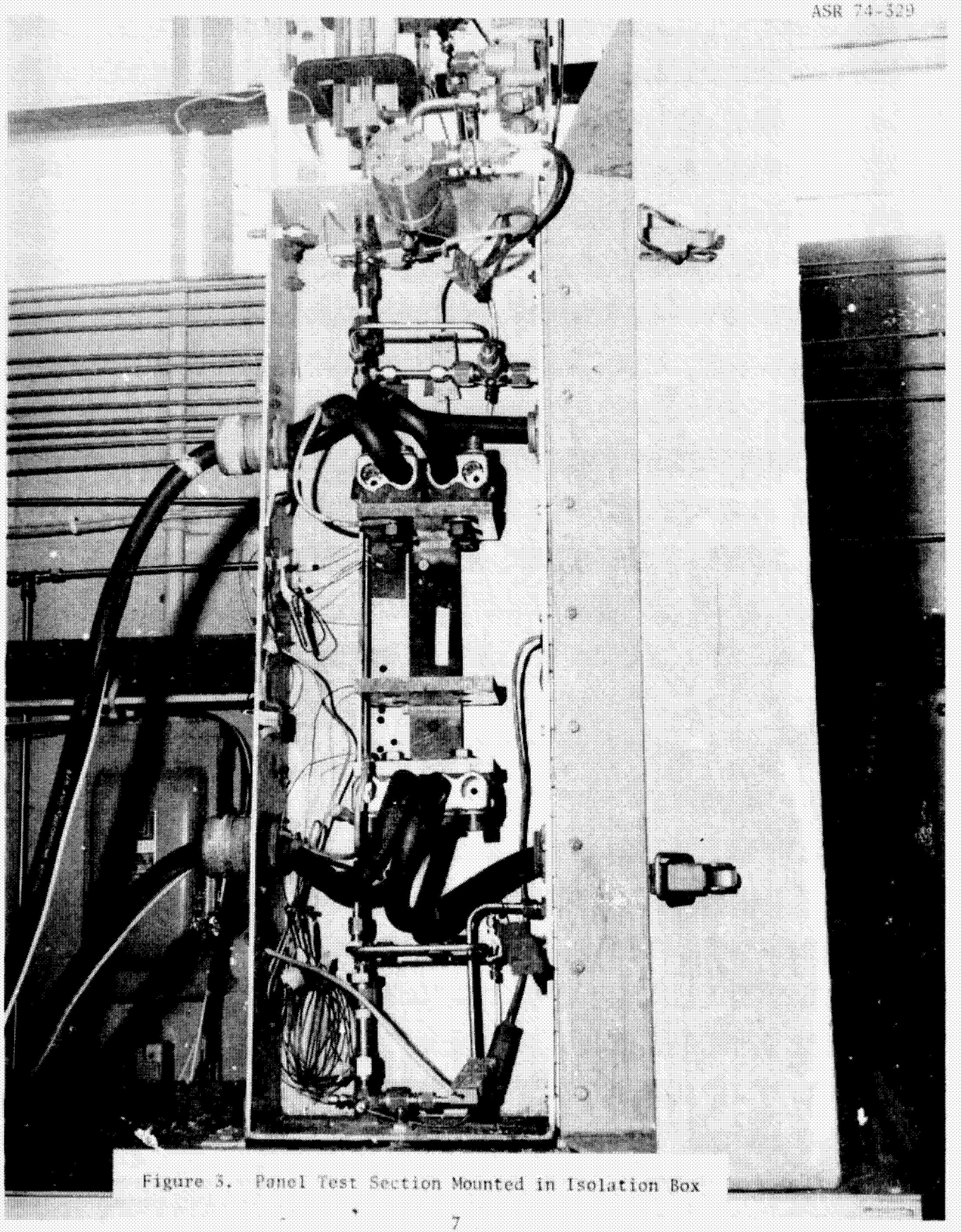

Figure 3. Panel Test Section Mounted in Isolation Box

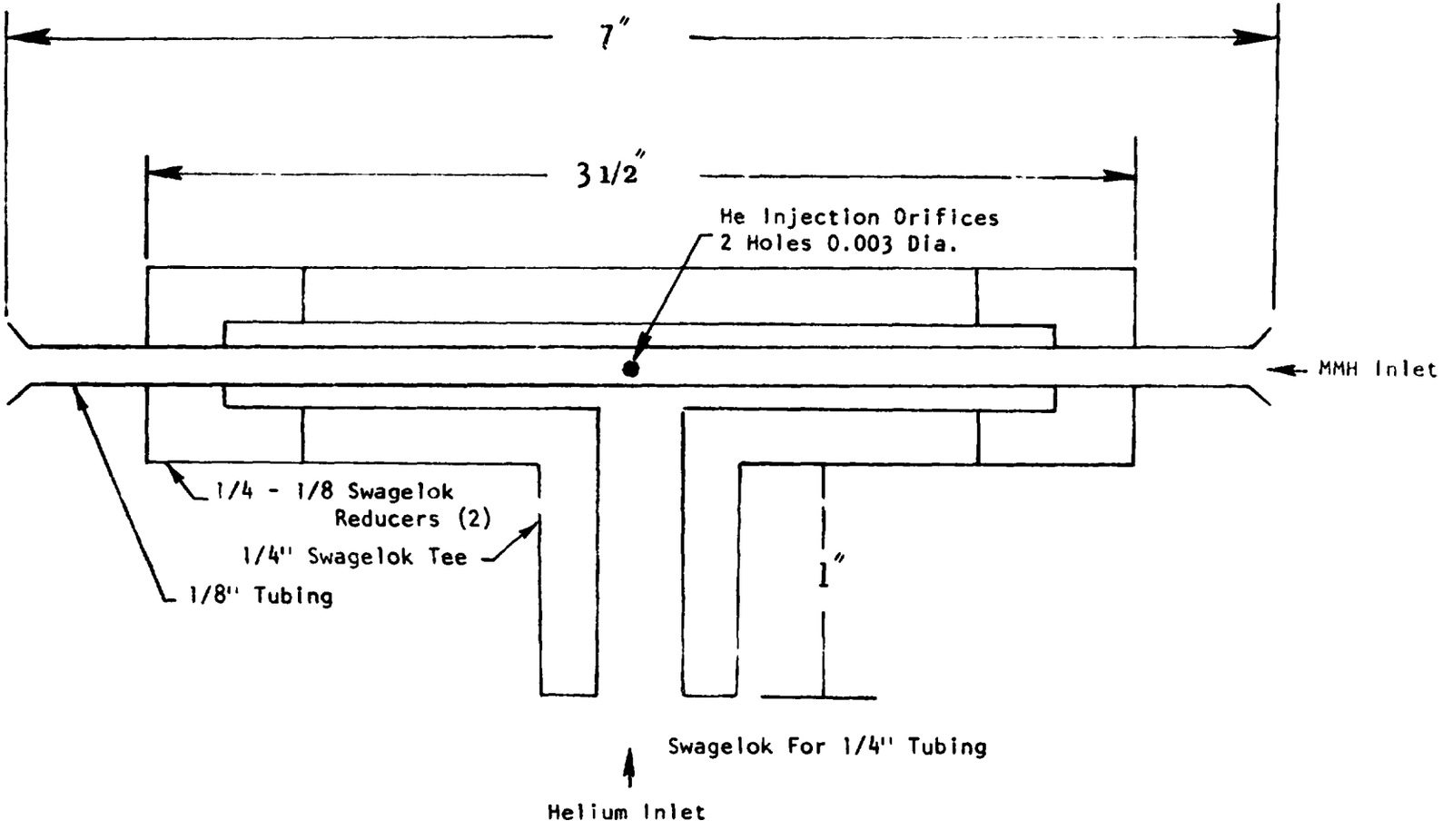

Figure 4. Helium Mixing "T"

pressure to accurately simulate flow of a slug of helium through a regeneratively cooled thrust chamber.

Instrumentation parameters, ranges, and display forms are listed in Table 1 A schematic of instrumentation locations is given in Fig. 5 for the three channel panel test section.

TEST HARDWARE

Test hardware consisted of circular tube, single rectangular channel, and three channel panel assemblies. The tube burnout and helium ingestion tests were conducted in a 0.125-inch O.D., 0.069-inch I.D., CRES 321 tube. The nominal heated test section lengths were 8.9 and 4.0 inches. Copper terminal blocks are brazed to the tube as shown in Fig. 6 to provide uniform electrical contact around the circumference of the tube. The terminal blocks are mounted to the micarta base, which has slotted holes to allow for thermal expansion.

The assembly for the two-dimensional heated tube tests consists of a ten-inch rectangular tube onto which circular tube ends are welded for flow connection. A copper strip is brazed to the tube along one surface. Voltage applied to the ends of the strip through the attached copper terminal blocks, as shown in Fig. 7, provides an asymmetric heat input to the tube which simulates heating of the hot wall of the chamber. The nickel close-out is not simulated because the back-wall material has been shown analytically to have little effect on the heat flux distribution in the area of the intersection of the hot wall and land. In addition, a nickel close-out on the test section would affect the electrical heat distribution.

Three copper terminal blocks were brazed to the rectangular test sections to provide for nominal heated lengths of 2.5, 6, and 9 inches. The maximum heated length of 9 inches was selected based on a predicted burnout heat flux (2-D) level of 4.2 Btu/in^2-sec corresponding to a velocity and subcooling of

TABLE 1. INSTRUMENTATION FOR ELECTRICALLY HEATED TUBE TESTS

Parameter	Symbol	Calibration Range	Display O - Oscillograph R - Pen Recorder P - Panel Gage or Meter * - Helium Tests only
Pressures, psia			
Coolant Orifice Inlet	PFS**	0-500	R
Coolant Orifice ΔP	DPF**	0-50	R
Tube Inlet	PTI**	0-500	R
Tube Outlet	PTO**	0-500	R
GHe Supply	PHS	0-3000	P*
GHe Orifice Inlet	PHI	0-500	P*
GHe Orifice ΔP	DPH	0-50	P*
Temperatures, F			
Coolant Orifice	TF**	60-100	P
Coolant Inlet	TFI**	60-100	P
Coolant Outlet	TFO**	60-400	O
Coolant Temp. Rise	ΔTC**	60-400	P
Tube Wall	TW1 TW2 TW3	60-2000	O (3), P (1)
GHe Orifice Inlet	THI	60-100	P*
Coolant Flowrate, cps	FC**		O, P
Tube Voltage	V	0-10	O, P
Tube Current, amps	I	0-6000	R, P
Automatic Cutoff		500-1500	P

** Denotes Two Measurements Required for Dual Flow Circuit Utilized in Panel Tests

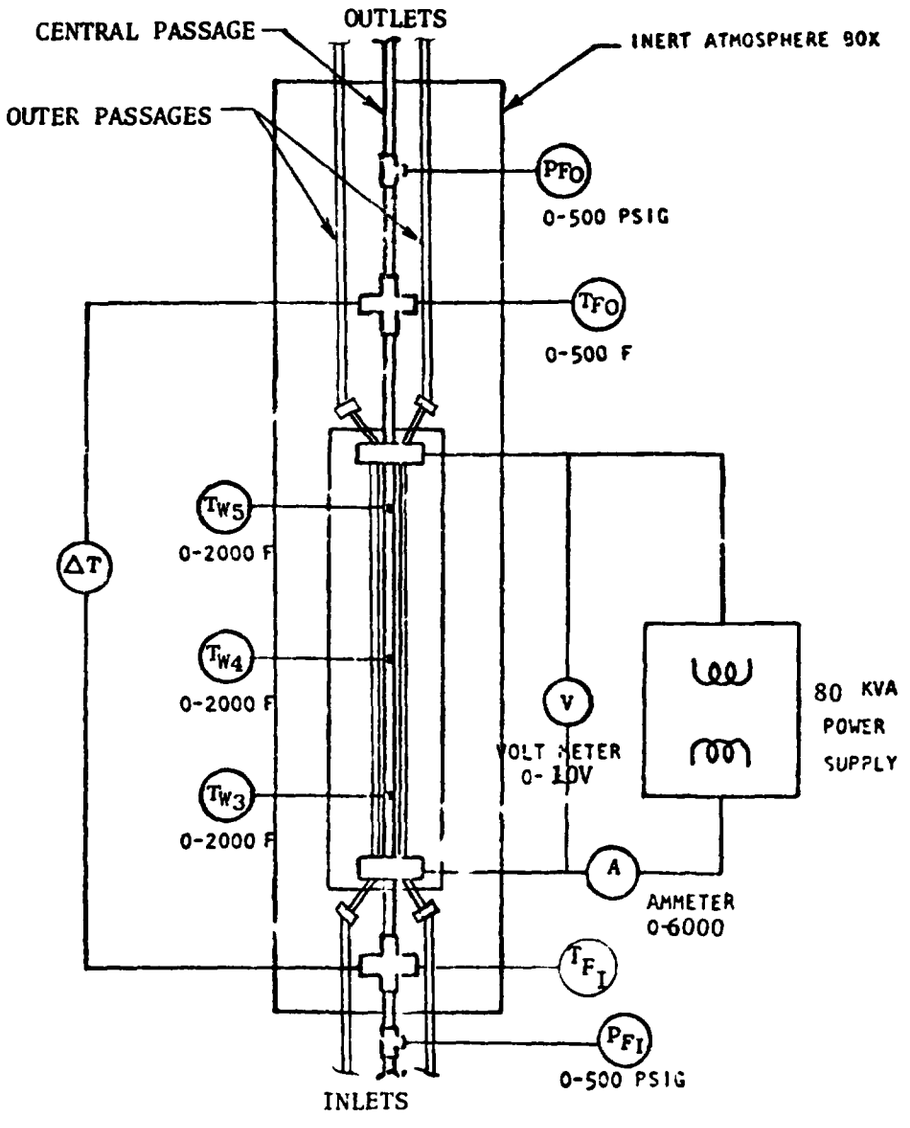

Figure 5. Three Passage Test Section Power Supply and Instrumentation

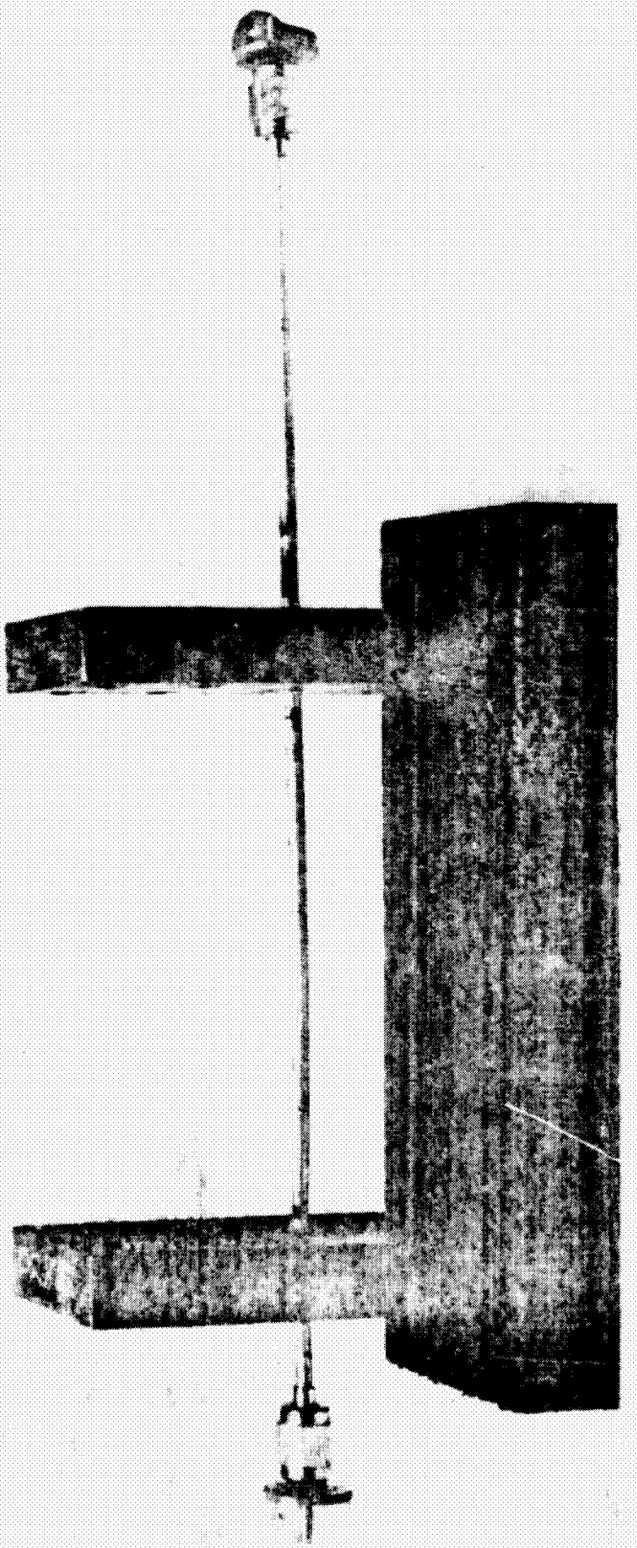

Figure 6. Heated Tube Assembly

Figure 7. 2-D Test Section

25.2 ft/sec and 131 F, respectively. These latter conditions represent normal design values in the Aerojet General SS/OME at a location 6.9 inches downstream of the injector. The short heated length of 2.5 inches simulates throat region velocity (15.6 ft/sec) and subcooling (217 F) at a predicted burnout heat flux (2-D) of about 4.0 to 4.5 Btu/in^2-sec.

Three test sections of two different cross-section geometries were fabricated and tested. One geometry was selected to simulate the Aerojet General OME channel design at a point 6.9 inches from the injector face. The other geometry represents an extreme 2-D geometry (wide land) to better evaluate geometry effects. The pertinent channel dimensions are noted in Table 2.

The 3-channel panel is constructed in a similar manner to the single channel test sections and is shown in Fig. 8. The panel incorporates a flared region on each end into which tubes (flattened on one end) are inserted and brazed in order to achieve individual flow control of each channel. This is shown pictorially in Fig. 9. Two panels of different channel geometry were fabricated and tested. One panel channel geometry was identical to the single channel geometry simulating the AJG OME coolant passage design discussed previously. The other panel geometry simulates a 10 inch diameter (ε_c = 3) combustor with a constant width land (straddle mill cutter design). The narrow land (0.040 inch) was selected to eliminate 2-D conduction effects. The panel channel geometries are also noted in Table 2.

TABLE 2. TEST SECTION GEOMETRY

Test Section Description	Channel Width (in.)	Channel Height (in.)	Land Width (in.)	*Heated Lengths (in.)	Comments
Channel #4A & 4B	0.141	0.046	0.073	9,6,2.5	AJG Geometry
Channel #5	0.064	0.046	0.150	9,6,2.5	Extreme 2-D Simulation
Panel #1 & 2	0.141	0.046	0.073	9,6,215	AJG Geometry
Panel #3	0.228	0.075	0.040	9,6,2.5	Straddle Mill 10 in. Diameter Combustor Simulation

Test Sections Have 3 Terminal Bars (Longest Length Simulates Combustor Subcooling, Shortest Length Simulates Throat Subcooling)

Note: All test sections have a 347 CRES hot-wall and closeout - 0.035 inch thick (nominal).

Figure 8. Three Channel Panel Test Section

ASR 74-329

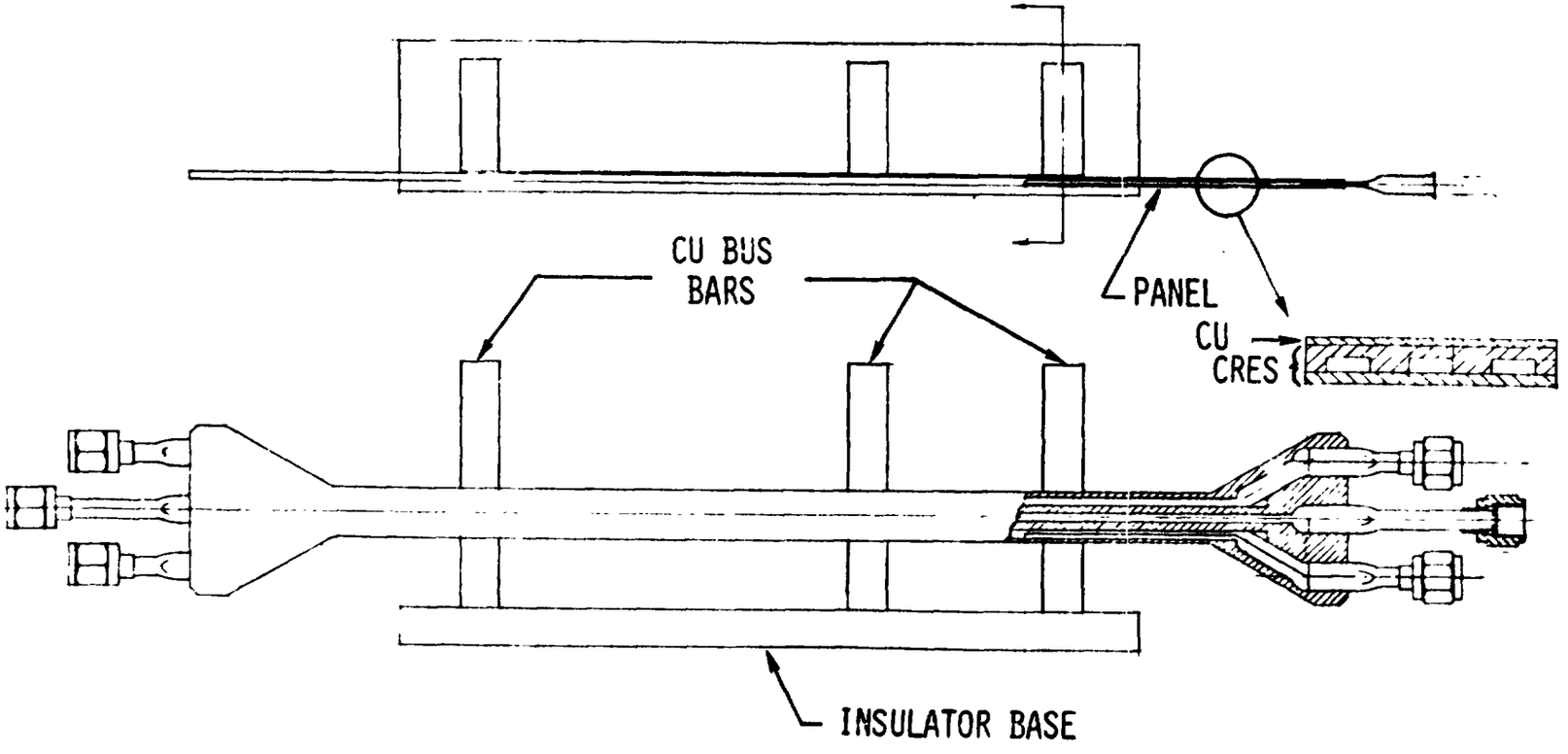

Figure 9. Electrically Heated Panel 3-Channel Simulator

TEST PROCEDURE

Pretest Calibration and Checkout Procedures

The coolant flowmeters were calibrated in water. The coolant flow measuring orifices were calibrated in water and checked against the flowmeters in MMH. The helium flow orifice was calibrated in helium using the displacement technique in an inverted beaker. The quality of the froth and the bubble characteristics were checked visually through a glass viewing section. Instrumentation calibrations, in terms of galvonometer deflections for the oscillograph recorder, were checked periodically during the test program.

Burn-Out Tests

The burn-out type tests in both the tube and single rectangular channel were conducted by first establishing the MMH flowrate (higher than the expected burn-out value) at the desired back pressure setting. The power level was then increased to the desired test value. The MMH coolant flowrate was then reduced gradually until a sudden increase in wall temperature occurrred indicating transition to film boiling. The power was cut automatically as the wall temperature exceeded the preset cut-off value (usually 1200 F).

In the case of panel burnout type tests the flowrate was maintained constant (due to the difficulty of reducing flowrate in both circuits simultaneously) and the power increased gradually until a sudden wall temperature increase occurred.

Helium Froth Burn-Out Tests

The helium pressure was set to provide the desired flowrate through the calibrated choked flow orifice (0.0017 inch diameter). The helium was then admitted to the test section through the mixing tee with the back pressure regulator set at the selected value (usually $\approx$ 170 psig). The charts were then turned on and the MMH flowrate established at a value higher than the expected burn-out level. The electric power was increased gradually to the

selected level. The MMH flowrate was then decreased slowly until a rapid wall temperature increase occurred and automatic power shut off initiated. The MMH flow and then the charts were shut down.

No helium froth tests were conducted with the panel test section.

Helium Bubble Tests

It was anticipated, at the time the test plan was written, that various discrete helium bubble tests would be conducted in the single rectangular channel and panel test sections. Subsequent deemphasis of bubble importance on chamber operation resulted in deletion of single channel bubble tests in favor of increased froth and 2-D burn-out testing. In addition, the initial panel tests indicated that a continuous helium flow (i.e., infinite bubble) could be maintained in the center channel at heat flux levels consistent with expected chamber values. This result eliminated the necessity of conducting finite bubble duration tests. The discrete bubble test procedure (used successfully in Task IX) is discussed in detail in the Task IX Test Report.

In the case of the infinite bubble tests (i.e., continuous helium flow) conducted with the 3-channel panel, the secondary valve (normally closed) was uncoupled and the primary valve (normally open) actuated to the closed position. The desired helium flow through the secondary circuit (to the center channel) was then established by helium tank pressure in conjunction with a choked flow orifice (0.0135 inch diameter).

Plugged Channel Tests

Two approaches were generally utilized to simulate plugged channel operation. Initially, nominal MMH flow was established in the outer channels with a small helium purge in the center channel. The power level was then increased until a rapid wall temperature excursion occurred and automatic power shutdown initiated.

The second technique started with nominal MMH flow in all three channels. The power was increased to the selected value. The flow in the center channel was then gradually decreased to zero with readings taken at various intermediate flow levels.

A third technique utilized only on the last test (No. 103) simulated downstream plugging. The center channel circuit was coupled to the outer channel circuit upstream of the test section (to simulate a common upstream manifold as in a thrust chamber). The center circuit was then blocked off downstream of the view tube after bleeding MMH into the center circuit to assure liquid trapped in the test section. Nominal MMH flow was then established in the outer channel circuit and power increased until a wall temperature excursion and automatic shutdown occurred.

POST-TEST HARDWARE STATUS

During test No. 33 (9 inch heated length tests) Channel Test Section No. 4A (AJG geometry) overheated resulting in localized melting of the copper heating strip and braze joint between the CRES channel and closeout. Repair of the braze joint leak (easily accomplished) would permit use of this test section in the 2.5 inch heated length position. (Repair of the copper heating strip is not recommended due to difficulty of assuring continuity, uniform thickness, and good bond to the CRES channel section.)

During test No. 93 (9 inch heated length test) Panel No. 3 overheated due to failure of the automatic cut-off device. The copper heating strip melted locally but the channel section remained intact. The test section was subsequently utilized in the 2.5 inch heated length test position.

Channel test sections No. 4B (AJG geometry), No. 5A (extreme 2-D geometry) and Panel No. 1 (AJG geometry) suffered no damage during test and can be utilized in any of the three heated length test positions. The tubular test section was also undamaged.

Panel No. 2 is identical to, and was intended as a backup for, Panel No. 1. This panel was not completed due to successful testing of Panel No. 1. All parts have been machined and only final assembly brazing is necessary to complete Panel No. 2.

DATA ANALYSIS

Burn-Out Tests

The electrical power, coolant outlet temperature and pressure, and coolant flowrate were obtained from the oscillographs and pen recorders at a point in time just prior to the recorded wall temperature increase indicating transition to film boiling. The outlet temperature and pressure were utilized to determine outlet subcooling. The coolant velocity was calculated from measured coolant flow and known test section flow area. The net heat input was calculated from the electrical power input minus the heat loss due to conduction, convection and radiation (as determined from heat loss calibrations without coolant flow). The net heat input was compared with that absorbed by the coolant to determine the overall test heat balance.

In the case of the symmetrically heated round tube, the effective heat flux was obtained from the net heat input divided by the internal surface area. For the rectangular channel and panel tests, however, the asymmetric heat flux equivalent to thrust chamber heating conditions was determined using a two-dimensional thermal conduction model. The equivalent 1-D heat flux is essentially the total heat generation (minus heat loss) minus the heat generated in the lands and closeout, divided by the width (lands plus channel) of the test section. In general, this heat flux level is about 10-15 percent lower than if it were assumed that all of the heat generation occurred in the copper strip and none in the CRES section.

Helium Froth Burn-Out Tests

Data analysis of froth burn-out tests is essentially the same as non-froth tests. The primary difference is that the coolant velocity is calculated according to the density of the helium-MMH mixture based on the volume percent of helium at inlet temperature conditions. The use of inlet temperature conditions, rather than outlet temperature, implies that there is negligible heat transfer from the MMH to the helium bubbles in the test section. The use of outlet temperature conditions in calculating helium volume percent would tend to increase the local coolant velocity by about 5 percent at the most for the conditions tested.

Panel Tests

In the case of the 3-channel panel burn-out tests, the center and outer channel conditions were not always identical. The approach taken in the burn-out tests was to obtain the weighted average velocity and subcooling of the center and outer channels in conjunction with the heat flux when transition to film boiling occurred.

For the plugged channel tests in which the center channel MMH flow was zero, the velocity and subcooling of the outer channels only were utilized in relation to the experimentally determined burn-out heat flux.

TEST RESULTS

Round Tube Tests

A total of 19 tests were conducted with MMH in a circular CRES tube. These tests consisted of 2 power calibration runs, 8 non-froth burn-out type tests, and 9 burn-out type tests with various amounts of helium ingested as a simulated froth. The non-froth tests were conducted to essentially checkout the heated tube test facility and provide a reference for the froth burn-out tests.

The round tube reduced test data are presen ed in Table 3. Heat flux levels ranged from about 1.6 to 6.5 Btu/in^2-sec. Coolant velocities ranged from 13 to 44 ft/sec with subcooling values of 38 to 159 F. The heat balance ranged from about 5 to 21 percent with an average overall heat balance of 11.8 percent for the 17 tests which underwent transition to film boiling.

The non-froth burn-out tests are compared in Fig. 10 with all of the previous round tube data taken at Rocketdyne under the contract and an earlier IR&D program. The new data are in excellent agreement with that taken previously. A best-fit curve is shown drawn through the data for use as a reference for helium ingestion, channel and panel tests. This curve is not the same as that used in the Rocketdyne OME regeneratively cooled chamber designs. The design curve essentially followed the lower bound (rather than the average) of the burnout heat flux data. The design curve is denoted by the dashed line in Fig. 10.

The helium ingestion tests were conducted with the same technique utilized previously in Task IX (see Test Procedures). Photographs of the MMH flow with various amounts of ingested helium, as taken through the downstream vertical sight tube, are presented in Fig. 11. It should be noted the resultant flow is not truly a froth but rather consists of small discrete bubbles of helium. This is similar to that reported in Task IX. It has been referred to as a froth primarily to distinguish these tests from the large discrete or continuous helium bubble tests.

Comparison of the froth results with the zero-helium-ingestion round tube tests is presented in Fig. 12. The limited data taken previously (Task IX) is also included for comparison. There appears to be a distinct degradation in the MMH burno it heat flux capability due to helium ingestion. The burnout heat flux capability is reduced about 15-20 percent. The relative amount of helium ingested does not appear to be a significant factor. Small amounts of helium ($\approx$ 5 percent by volume) appear to degrade the burnout heat flux as much as larger amounts ($\approx$ 20 percent) except, perhaps, at the higher heat flux level.

TABLE 3. ROUND TUBE TEST DATA SUMMARY

	1 Test No.	2 Heated Length (in.)	3 Test Type	4 Heat Flux (Btu/in^2-sec)	5 MMH Flowrate (lb/sec)	6 MMH Outlet Temperature (F)	7 MMH Inlet Temperature (F)	8 ** Heat Balance (%)	9 MMH Outlet Pressure (psig)	10 Outlet Subcooling ΔT_{Sub} (F)	11 Helium Volume Percent @ Inlet	12 Coolant Velocity (ft/sec)	13 $V \cdot \Delta T_{Sub}$ $\left(\frac{Ft-F}{sec}\right)$	14
1	1	8.9	Checkout											
2	2		Checkout											
3	3		*B.O.	1.64	0.016	295	77	21.1	175	74	0	13.2	980	
4	4			2.25	0.021	317	78	16.9	175	52	0	17.7	920	
5	5			2.28	0.023	328	79	8.8	170	38	0	19.3	730	
6	6	4.0		2.88	0.016	285	78	5.3	180	86	0	13.1	1130	
7	7			4.16	0.023	261	78	16.5	180	110	0	18.4	2030	
8	8			5.18	0.038	237	78	5.1	183	136	0	29.6	4020	
9	9			6.55	0.055	215	78	5.1	185	159	0	42.5	6760	
10	10		Froth B.O.	2.94	0.017	242	77	21.4	165	122	6.4	14.4	1750	
11	11			3.00	0.018	242	77	20.6	165	122	12.0	15.7	1920	
12	12			2.94	0.018	237	77	19.2	170	129	16.7	17.0	2200	
13	13			4.14	0.033	222	77	6.1	170	144	7.1	27.2	3920	
14	14			4.22	0.029	230	77	13.3	170	136	14.6	26.5	3610	
15	15			4.09	0.029	235	78	8.3	170	131	20.3	28.6	3750	
16	16			5.36	0.045	210	78	8.7	170	156	8.3	37.8	5900	
17	17			5.34	0.044	218	78	4.9	170	148	15.7	40.5	5990	
18	18			5.32	0.045	213	78	5.8	170		21.3	44.1	6750	
19	19		B.O.	5.32	0.036	238	79	11.2	170		0	28.4	3640	
20														
21														
22														
23														
24														
25														

* Denotes transition to film boiling (burn-out)

** Heat balance = $\left(1 - \frac{Q_{Out}}{Q_{In}}\right) \times 100$

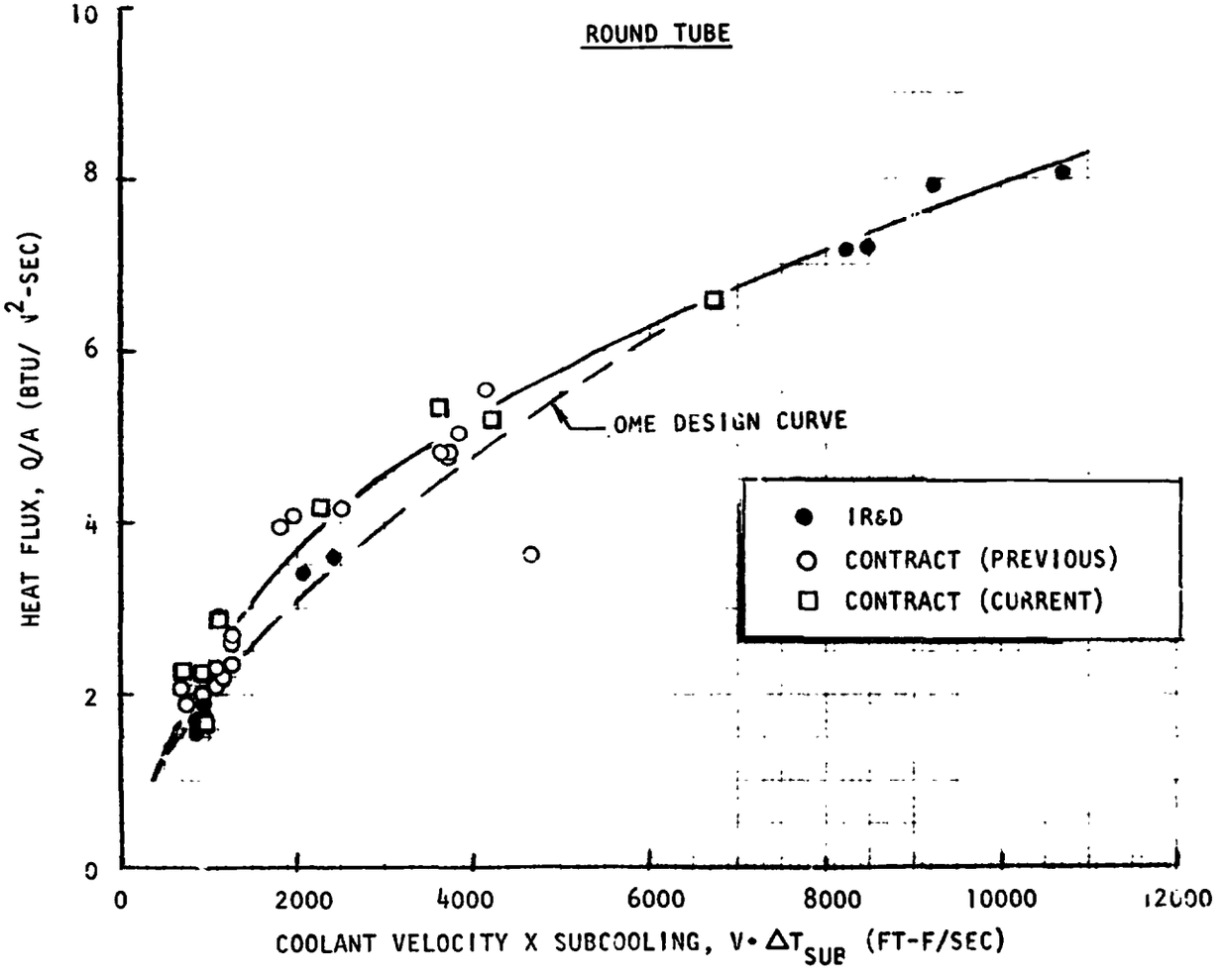

Figure 10. Experimental Burnout Heat Flux Data for MMH

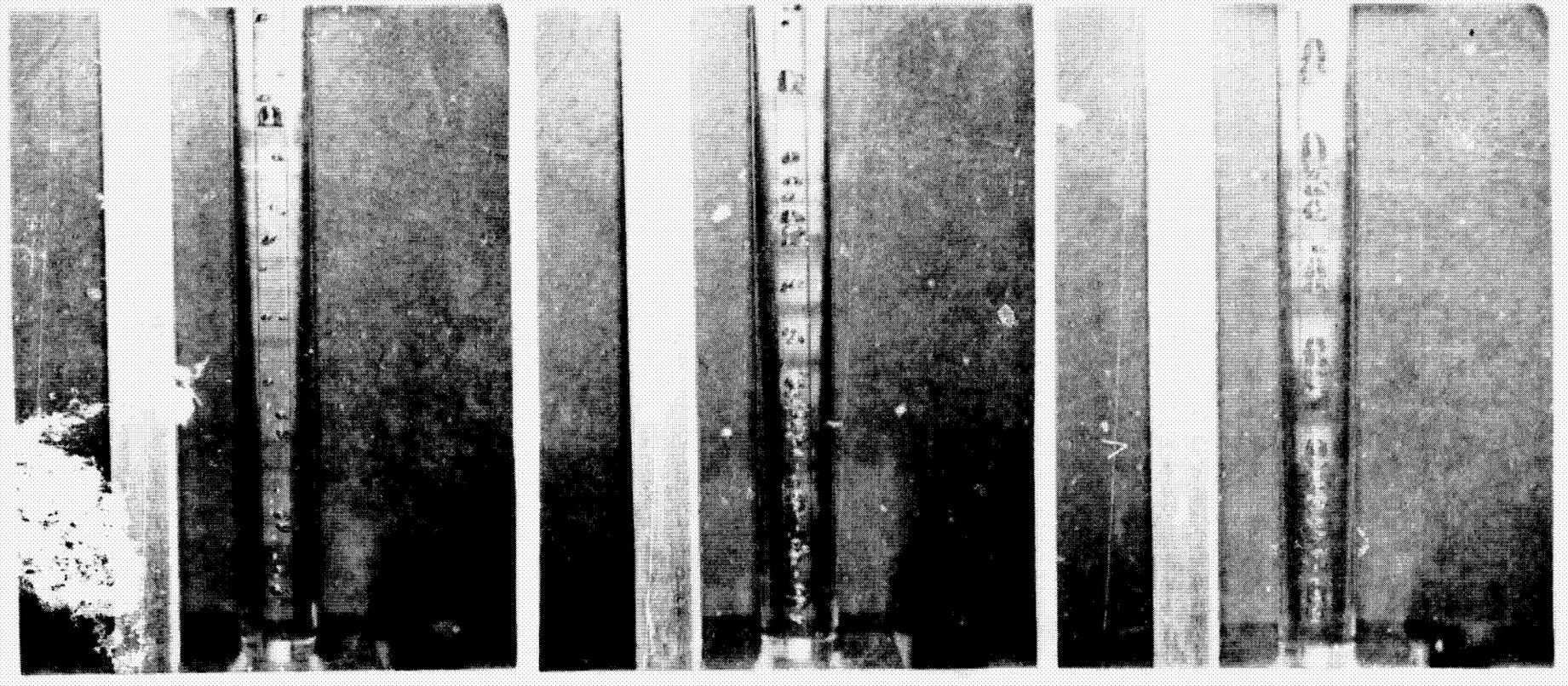

5% (BY VOLUME) 15% (BY VOLUME) 30% (BY VOLUME)

Figure 11. Helium Froth Flows as Viewed Through Downstream Vertical Sight Tube

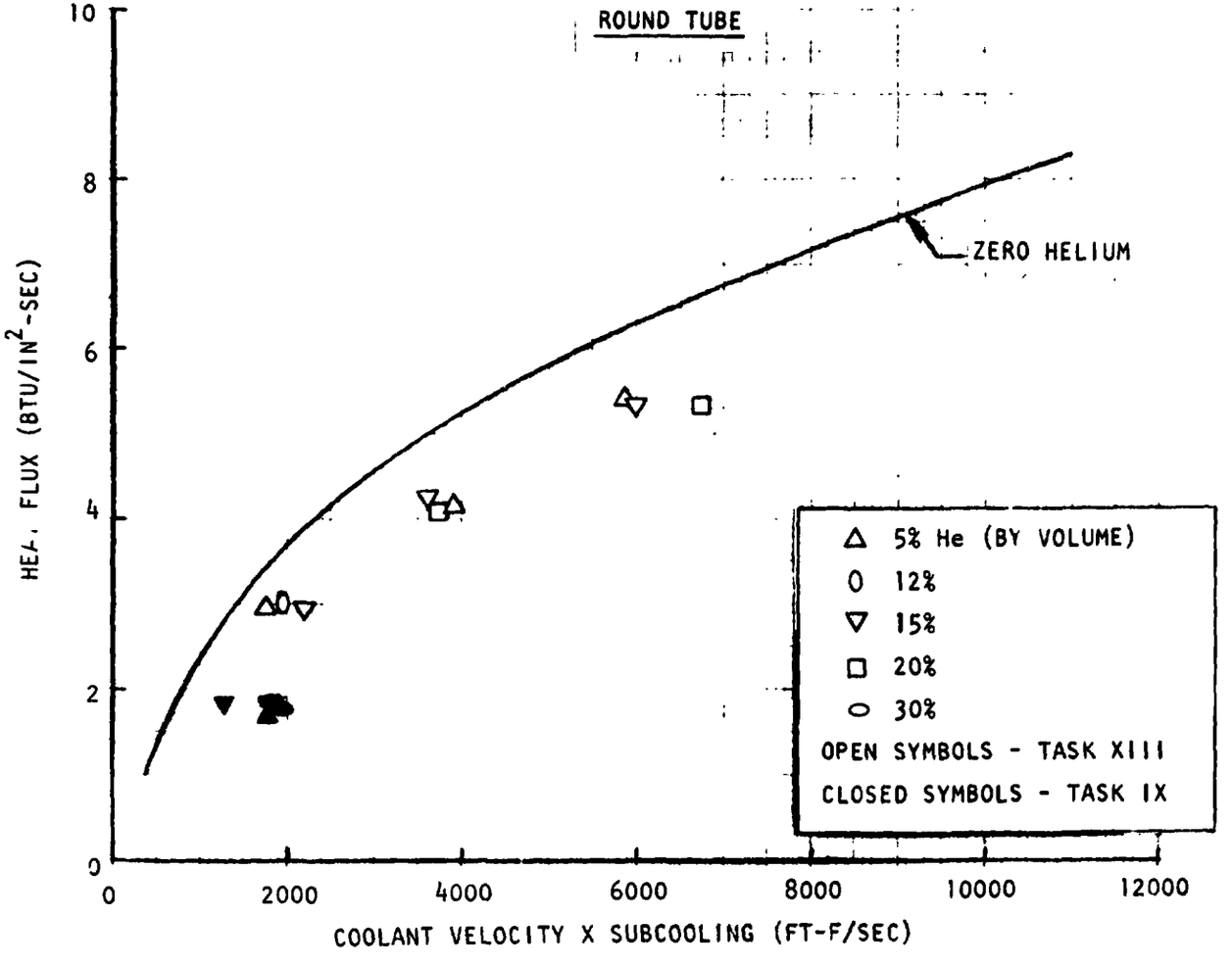

Figure 12. Effect of Helium Ingestion on Burnout Heat Flux of MMH

The reason for the cooling degradation is not clear. It is possible that the relatively large diameter helium bubbles inhibit the heat and mass transfer between the liquid MMH and the small MMH vapor bubbles formed during the nucleate boiling process. This would tend to reduce the effective subcooling resulting in transition to film boiling at a lower heat flux level. Further effort is required in this area to fully understand the cooling mechanism involved.

Channel Tests

Extensive testing was conducted with asymmetrically heated single channels. Two distinct geometries and two heated lengths were evaluated. The primary geometry (channels No. 4A and 4B) was selected to match the coolant passage geometry in the Aerojet General OME regeneratively cooled chamber at a point 6.9 inches downstream of the injector face specified as the most critical location. The heated length of 9.0 inches (actually 8.5 inches effective after adjusting for the intermediate terminal block in which no electrical heating occurs) was selected to provide the design subcooling (131 F) at the predicted 2-D burnout heat flux level of 4.2 Btu/in^2-sec. The effective 1-D hot gas heat flux is 3.0 Btu/in^2-sec. The 2.5 inch heated length was selected to match throat subcooling conditions (217 F) at throat design velocity ($\approx$ 15 ft/sec).

The alternate channel geometry (channel No. 5A) was selected primarily to provide additional data on 2-D conduction effects. A wide land (0.150 inch) was utilized to provide an extreme 2-D conduction geometry. Heated lengths were maintained at the same values as channels No. 4A and 4B to facilitate data comparison and hardware installation.

The reduced data for all of the channel tests are summarized in Table 4. The results of the 9 inch heated length channel tests are compared with the round tube (1-D) results in Fig. 13. It is apparent that, except at low $V \cdot \Delta T_{sub}$ values where considerable tube data scatter exists, there is a significant reduction in the effective 1-D burnout heat flux due to 2-D conduction effects. As would be expected, the extreme 2-D geometry (wide land), shows the largest degradation in effective burnout heat flux capability.

The predicted burnout heat flux levels for the two geometries agree favorably with the experimental data as noted in Fig. 13. The analytical prediction is based on a 2-D conduction analysis as discussed in the Appendix of the Task IX Test Report (Rocketdyne ASR 74-131). The assumed superheat of 50 F refers

TABLE 4. SINGLE RECTANGULAR CHANNEL TEST DATA SUMMARY

	1 Test No.	2 Test Section	3 Heated Length (in.)	4 Test Type	5 *Adjusted Heat Flux $\left(\frac{Btu}{in^2\text{-}sec}\right)$	6 MMH Flowrate (lb/sec)	7 MMH Outlet Temp. (F)	8 MMH Inlet Temp. (F)	9 Heat Balance (%)	10 MMH Outlet Pressure (psig)	11 Outlet Sub-cooling ΔT_{SUB} (F)	12 Helium Volume Percent @ Inlet	13 Coolant Velocity (ft/sec)	14 $V \cdot \Delta T_{SUB}$ $\left(\frac{ft\text{-}F}{sec}\right)$	15	16	17	18	19	20
															Remarks					
1	20	4A	9.0	Checkout																
2	21			Checkout																
3	22			B.O.	1.80	0.020	313	76	8.2	176	56	0	9.7	545						
4	23			Froth - B.O.	1.82	0.023	287	77	7.2		82	9.8	12.1	990						
5	24				1.76	0.023	277	77	9.1		92	19.8	13.5	1240						
6	25				1.76	0.022	285	77	9.1		84	30.5	15.0	1260						
7	26			B.O.	2.65	0.046	246	77	2.5		123	0	20.1	2475						
8	27			Power Calibration	--	--	--	--	--	--	--	--	--	--						
9	28			B.O.	2.87	0.049	243	74	0.3	176	126	0	22.1	2785						
10	29			Froth - B.O.	2.77	0.046	241	74	3.1		128	5.8	22.3	2855						
11	30				2.87	0.052	226	75	4.7		143	10.4	26.1	3735						
12	31				2.90	0.052	236	75	0.4		133	15.8	27.8	3695						
13	32			B.O.	3.45	0.062	241	76	-1.1		128	0	28.0	3585						
14	33			Froth - B.O.	3.57	0.062	241	76	2.7		128	~ 5.7	29.7	3800	Test section failed - flow reduced too fast					
15																				
16	34	4B	9.0	B.O.	--	--	--	--	--	--	--	--	--	--	Isolation box window fogged - test terminated					
17	35				--	--	--	--	--	--	--	--	--	--	Low heat flux - no burnout					
18	36				2.07	0.030	247	71	7.5	95	73	0	13.5	985						
19	37				2.85	0.053	221	71	-2.2		99	0	23.7	2345						
20	38				3.73	0.072	216	71	-0.5		104	0	32.2	3350						
21																				
22	39	4B	2.5	B.O.	--	--	--	--	--	--	--	--	--	--	Low heat flux - no burnout					
23	40				2.82	0.011	255	86	17.9	169	111	0	5.1	565						
24	41				2.97	0.014	226	87	21.4	165	138	0	6.1	840						
25	42			Froth - B.O.	3.17	0.019	199	87	18.9		165	4.8	8.6	1410						
26	43				3.30	0.023	184	87	16.0		180	12.5	11.4	2055						
27	44				3.25	0.019	204	87	15.8		160	39.5	13.9	2225						
28	45			B.O.	3.80	0.031	173	87	14.0	173	195	0	13.4	2615						
29	46			Froth - B.O.	--	--	--	--	--	--	--	--	--	--	Auto cut before stabilized					
30	47			Froth - B.O.	3.92	0.033	176	87	8.2	165	188	6.4	15.3	2870	Repeat Test No. 46					
31	48			Froth Movies	--	--	--	--	--	--	--	Varied	--	--	Movies of various He ingestion levels					
32																				
33	* Adjusted for equivalent 1-D heat flux - does not include heat generation in lands or closeout																			
34																				
35																				

TABLE 4. (Concluded)

	1 Test No.	2 Test Section	3 Heated Length (in.)	4 Test Type	5 *Adjusted Heat Flux ($\frac{Btu}{in^2-sec}$)	6 MMH Flowrate (lb/sec)	7 MMH Outlet Temp. (F)	8 MMH Inlet Temp. (F)	9 Heat Balance (%)	10 MMH Outlet Pressure (psig)	11 Outlet Sub-cooling ΔT_{SUB} (F)	12 Helium Volume Percent @ Inlet	13 Coolant Velocity (ft/sec)	14 $V \cdot \Delta T_{SUB}$ ($\frac{ft-F}{sec}$)	15 16 17 18 19 20 Remarks
1	49	4B	2.5	Checkout											Power calibration
2	50			Checkout											Power calibration
3	51			B.O.	2.95	0.008	299	73	23.6	172	69	0	3.8	265	
4	52			Froth - B.O.	3.08	0.017	196	73	18.7		172	19.6	9.0	1540	
5	53			B.O.	4.35	0.039	157	71	6.9		211	0	16.7	3520	
6	54			Froth - B.O.	3.83	0.025	186	74	12.1		182	31.6	15.6	2845	
7	55				4.62	0.042	157	74	9.1		211	6.4	19.2	4060	
8	56				4.37	0.039	158	75	10.4		210	5.6	17.7	3715	
9	57			B.O.	4.45	0.042	167	88	9.9	173	201	0	17.8	3585	
10	58			Froth - B.O.	4.35	0.040	167	88	13.0	172	201	5.7	18.0	3625	
11															
12	59	5A	9.0	B.O.	1.55	0.014	333	71	12.9	165	31	0	15.3	475	
13	60				--	--	--	--	--	--	--	--	--	--	Auto cut before stabilized
14	61				2.58	0.039	251	71	1.4	165	113	0	38.9	4390	
15	62				3.26	0.056	235	71	-2.4	169	131	0	55.8	7310	
16	63				--	--	--	--	--	--	--	--	--	--	Auto cut before stabilized
17	64				3.46	0.058	234	71	0	165	130	0	58.4	7590	
18	65				--	--	--	--	--	--	--	--	--	--	Auto cut before stabilized
19															
20	66	5A	2.5	B.O.	--	--	--	--	--	--	--	--	--	--	Low heat flux - no burnout
21	67				--	--	--	--	--	--	--	--	--	--	Low heat flux - no burnout
22	68				2.61	0.014	214	76	11.5	169	152	0	13.2	2010	
23	69				3.05	0.020	188		11.2	169	178	0	18.8	3345	
24	70				4.13	0.036	171		1.1	172	197	0	33.8	6650	
25	71				4.72	0.046	158		5.3	172	210	0	43.0	9020	
26															
27															
28															
29															
30															
31															
32															
33															
34															
35															

* Adjusted for equivalent 1-D heat flux - does not include heat generation in lands or closeout

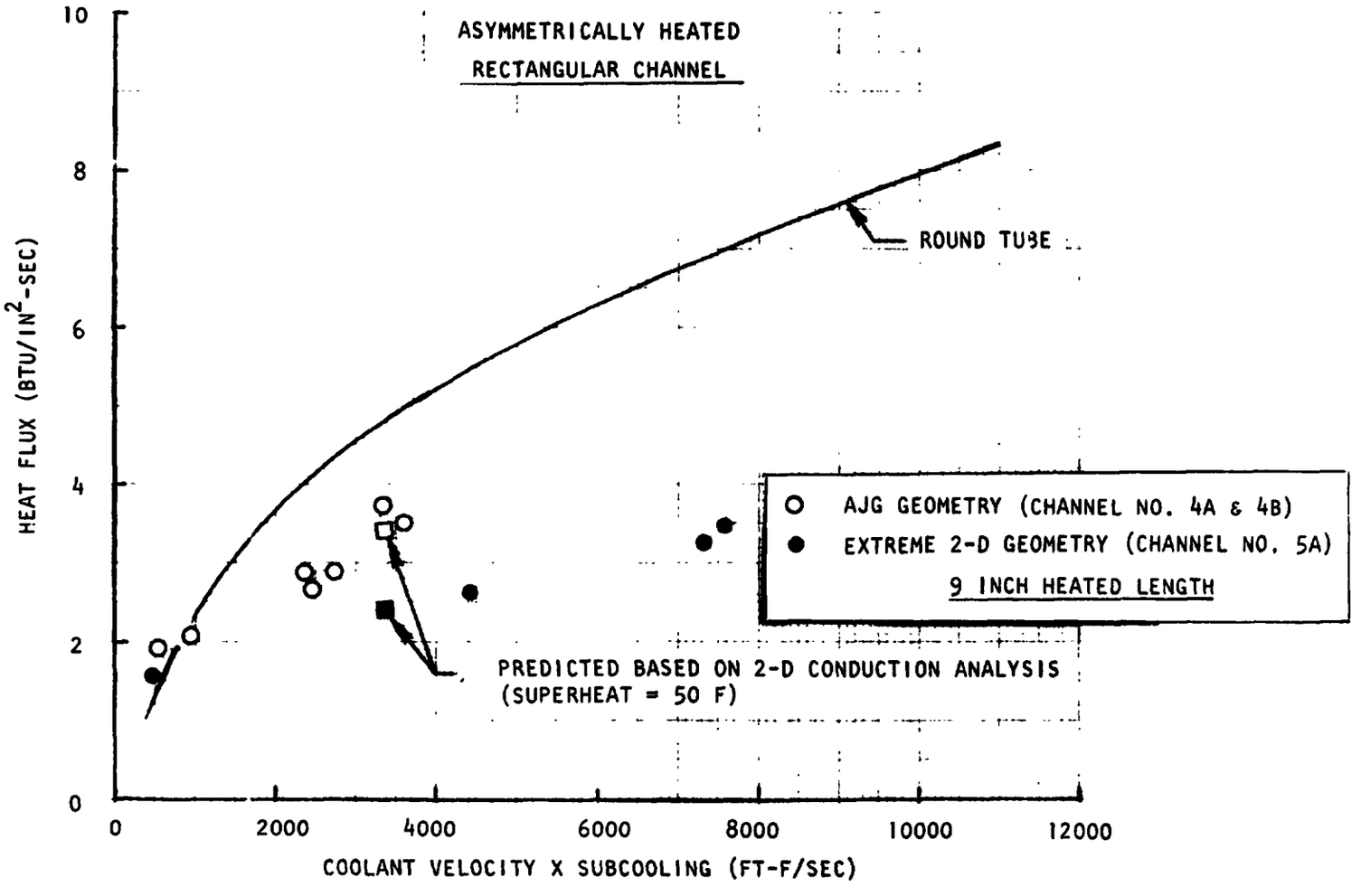

Figure 13. Experimental Burnout Heat Flux Data for MMH

to the maximum difference between the wall temperature and coolant saturation temperature when transition to film boiling occurs.

The results of the 2.5 inch heated length channel tests are compared with the round tube (1-D) results in Fig. 14. The reduction in burnout heat flux level is considerably less as compared to the 9 inch heated length tests. Indeed at the low $V \cdot \Delta T_{sub}$ values the AJG geometry appears capable of a higher heat flux than that based on a 1-D tube value. It is possible that the low coolant bulk temperature results in better cooling in the land region.

An analytical evaluation of the short heated length tests was not undertaken due to the fact that the channel geometry is not representative of that which would be used in the throat region of the chamber.

Helium ingestion tests were conducted in the AJG geometry channels only, at both heated lengths. These results are presented in Fig. 15. There appears to be a slight degradation in heat flux capability in some cases although not nearly as noticeable as in the case of the round tube tests. This may possibly be attributed, in some manner, to the non-uniform heating of the rectangular test sections. Again, the cooling mechanism with helium ingestion is unclear and warrants further study.

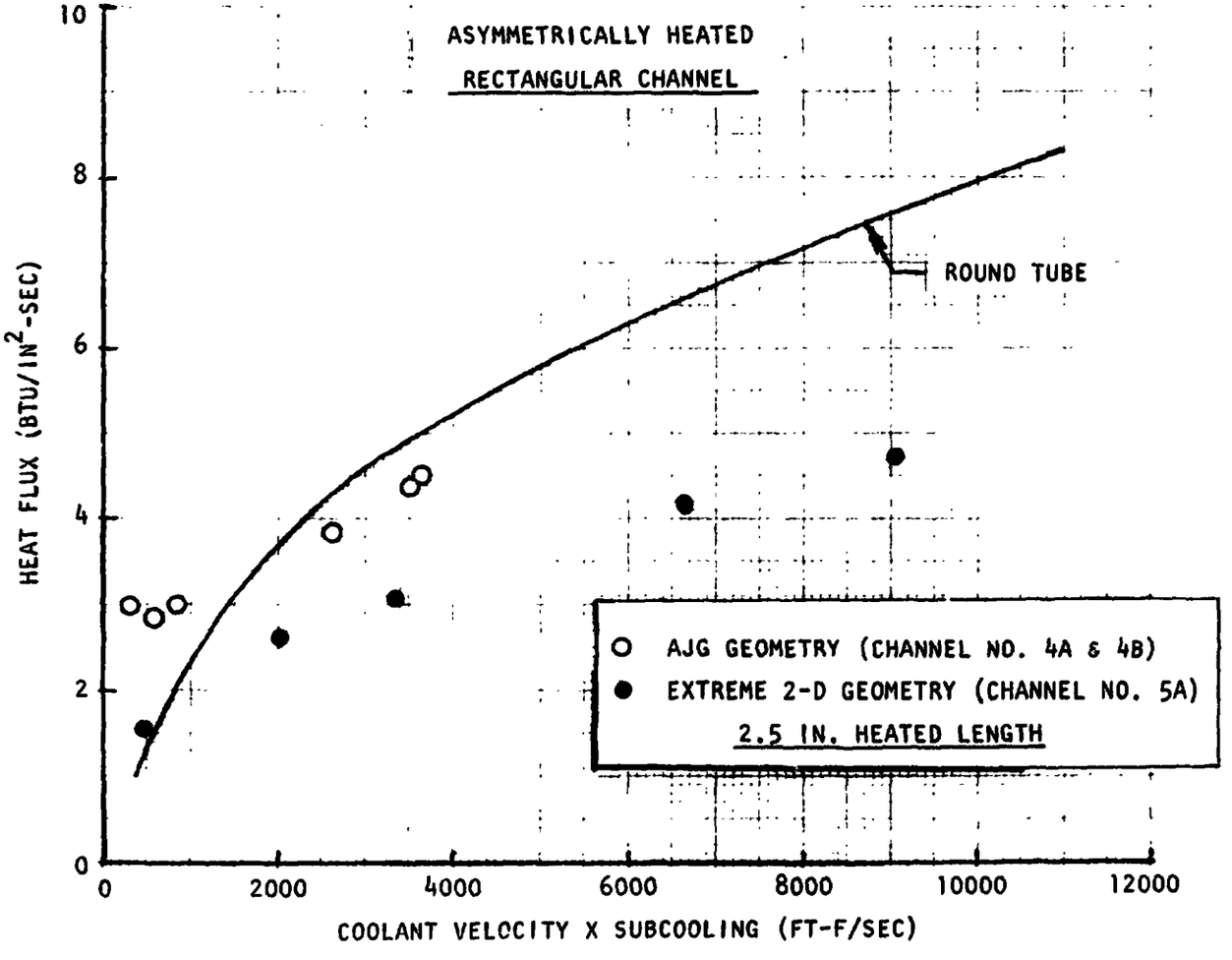

Figure 14. Experimental Burnout Heat Flux Data for MMH

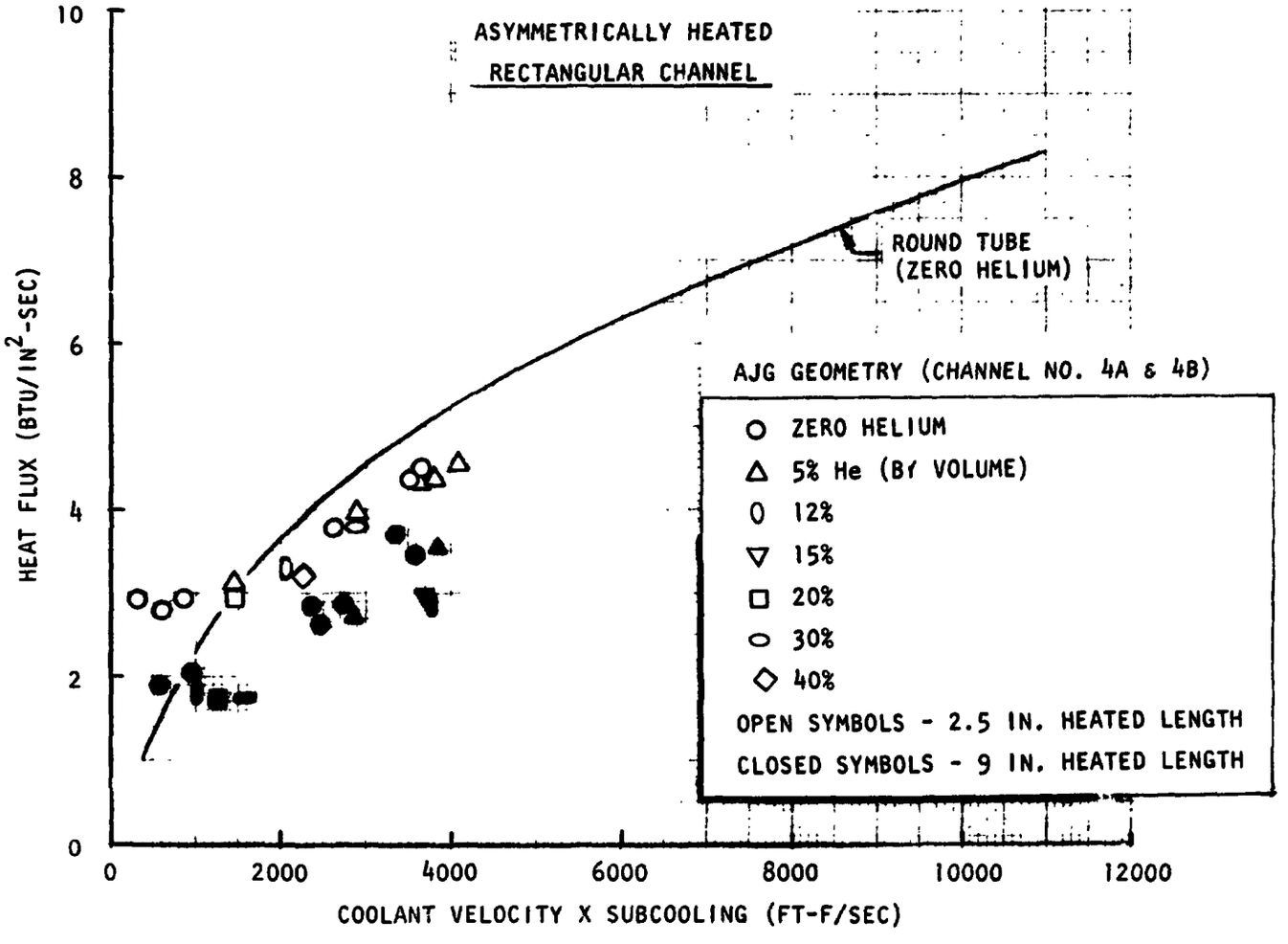

Figure 15. Effect of Helium Ingestion on MMH Burnout Heat Flux

Panel Tests

A total of 31 tests were conducted with MMH in two panels composed of three rectangular channels each. The channel geometry of each panel differed markedly as described in the Test Hardware section of this report. Three primary areas of interest were investigated experimentally: (1) helium bubble ingestion, (2) plugged channel simulation, and (3) simple burn-out type tests for comparison to single channel results. Both 9 inch and 2.5 inch heated lengths were tested to simulate combustor and throat region conditions, respectively. The reduced test data are presented in Table 5.

The simplest data to evaluate is that of the burnout type tests wherein the MMH flow was the same in all three channels. The results of these tests, in terms of burnout heat flux versus the familiar $V \cdot \Delta T_{SUB}$ parameter, is compared with the single channel test results in Fig. 16. It is apparent that there is excellent agreement between panel and single channel tests for both the 9 inch and 2.5 inch heated lengths. This result tends to support the validity of single channel tests.

Also included in Fig. 16 are the burnout heat flux test results for Panel No. 3. (Although the original test plan did not call for this type of test on Panel No. 3, a limited number of tests were conducted as time permitted.) The geometry of this panel is characterized by narrow lands and wide channels and is intended to simulate a 1-D conduction geometry in the combustion region of a 10 inch diameter combustor.

The results of the 9 inch Panel No. 3 tests are seen to fall on the 1-D (round tube) correlating curve. Due to the much larger cross section of Panel No. 3 sufficient electrical power could not be generated to verify the 1-D design at heat flux levels higher than about 1.5 Btu/in^2-sec. It should be noted that this heat flux level is about what would be expected for the 10 inch diameter combustor at nominal operating conditions.

TABLE 5. THREE CHANNEL PANEL TEST DATA SUMMARY

	1 Test No.	2 Test Section	3 Heated Length (in.)	4 Test Type	5 Adjusted Q/A $\left(\frac{Btu}{in^2\text{-}sec}\right)$	6 Center Channel Fluid	7 Center Channel Flow (lb/sec)	8 Outer Channels Total Flow (lb/sec)	9 TFI (F) Center/ Outer	10 Center TFO (F)	11 Outer TFO (F)	12 Heat Balance (%)	13 PFO (psig)	14 $\overline{\Delta T}_{SUB}$ (F)	15 $\overline{V}$ (ft/sec)	16 $\overline{V \cdot \Delta T}_{SUB}$ $\left(\frac{ft\text{-}F}{sec}\right)$	17	18	19 REMARKS	20	21
1	72	Panel #1	9.0	Infinite Bubble	1.90	He	.00115	0.087	75/75	395	236	5.0	172	132	20.0	2635					
2	73				1.99	He	.00115	0.087	73/73	353	235	9.1		133	20.0	2655					
3	74				1.35	He	.00115	0.050	80/80	393	281	2.3		87	11.5	[illegible]					
4	75			*P.C.	1.93	He	~.0002	0.0865	67/66	--	239	5.1		129	19.8	2560					
5	76				1.35	He	~.00015	0.0485	74/68	--	275	8.0		93	11.1	1035					
6	77				0.73	He	~.0001	--	--	--	--	--	--	--	--	--	Low TFO! Flow + [illegible]				
7	78				1.35	He	~.00015	0.061	80/68	--	231	9.2	95	89	14.0	1246					
8	79				1.36	He	~.00[illegible]	0.0615	82/68	--	224	8.4	95	96	14.8	1421					
9	80				2.0[illegible]	None	0	0.091	68/75	--	231	12.5	95	89	20.0	1859	No B.O.				
10	81			B.O.	1.66	None	.021	0.041	96/100	287	315	5.1	172	62	9.8	605					
11	82				1.57	None	.020	0.040	96/100	275	297	10.4		78	9.5	742					
12	83				2.08	None	.031	0.060	100/102	266	281	6.3		92	14.3	1313					
13	84				2.63	None	.044	0.0875	103/104	244	261	7.5		113	20.9	2353	Blown - no B.O.				
14	85				2.63	None	.045	0.092	103/104	262	273	-5.7		99	21.9	2167					
15																					
16	86	Panel #3	9.0	I.C.	1.30	He	~.0001	0.083	73/65	--	227	-0.9	172	141	7.4	1046					
17	87				1.12	He	~.0001	0.060	95/67	--	254	1.9	172	114	5.4	611					
18	88				1.20	He	~.0001	0.087	90/67	--	205	0.9	95	115	7.8	894					
19	89				1.00	He	~.0001	0.060	97/68	--	229	3.9		91	5.4	488					
20	90				1.17	None	0	0.087	67/67	--	206	-1.6		114	7.8	886	No. B.O.				
21	91			B.O.	1.05	None	.014	0.029	87/90	271	329	10.9	172	58	2.7	156					
22	92				1.48	None	.030	0.0615	93/94	250	258	1.8		113	5.7	644					
23	93				0.98	None	.0185	0.0365	93/94	248	272	6.4		104	3.4	352	Auto cut failed - cooler acted				
24																					
25	94	Panel #1	2.5	P.C.	2.47	He	~.0001	0.0655	/75	--	147	21.2	172	221	14.0	3100	No B.O.				
26	95			P.C.	2.55	None	0	0.0635	86/83	--	160	20.5		208	13.6	2828	No B.O.				
27	96			B.O.	3.38	None	.0175	0.0365	82/83	188	205	23.6		169	8.0	1352					
28	97			B.O.	3.07	None	.013	0.028	83/83	205	230	23.5		146	6.2	909					
29																					
30	98	Panel #3	2.5	P.C.	2.18	He	~.0001	0.087	88/75	--	130	27.5	172	238	7.3	1727	No B.O.				
31	99			P.C.	2.37	None	0	0.090	82/83	--	151	24.6		217	6.7	1448					
32	100			B.O.	2.60	None	.024	0.0495	81/84	155	162	29.0		208	4.1	852	No B.O.				
33	101				2.38	None	.018	0.034	85/85	176	192	27.1		183	2.9	537	No B.O.				
34	102				2.45	None	.0135	0.0265	90/91	217	234	26.2		140	2.3	323					
35	1[illegible]			F.C.	2.50	None	0	0.089	88/89	--	165	10.8		203	7.4	1502					

* Plugged center channel simulation

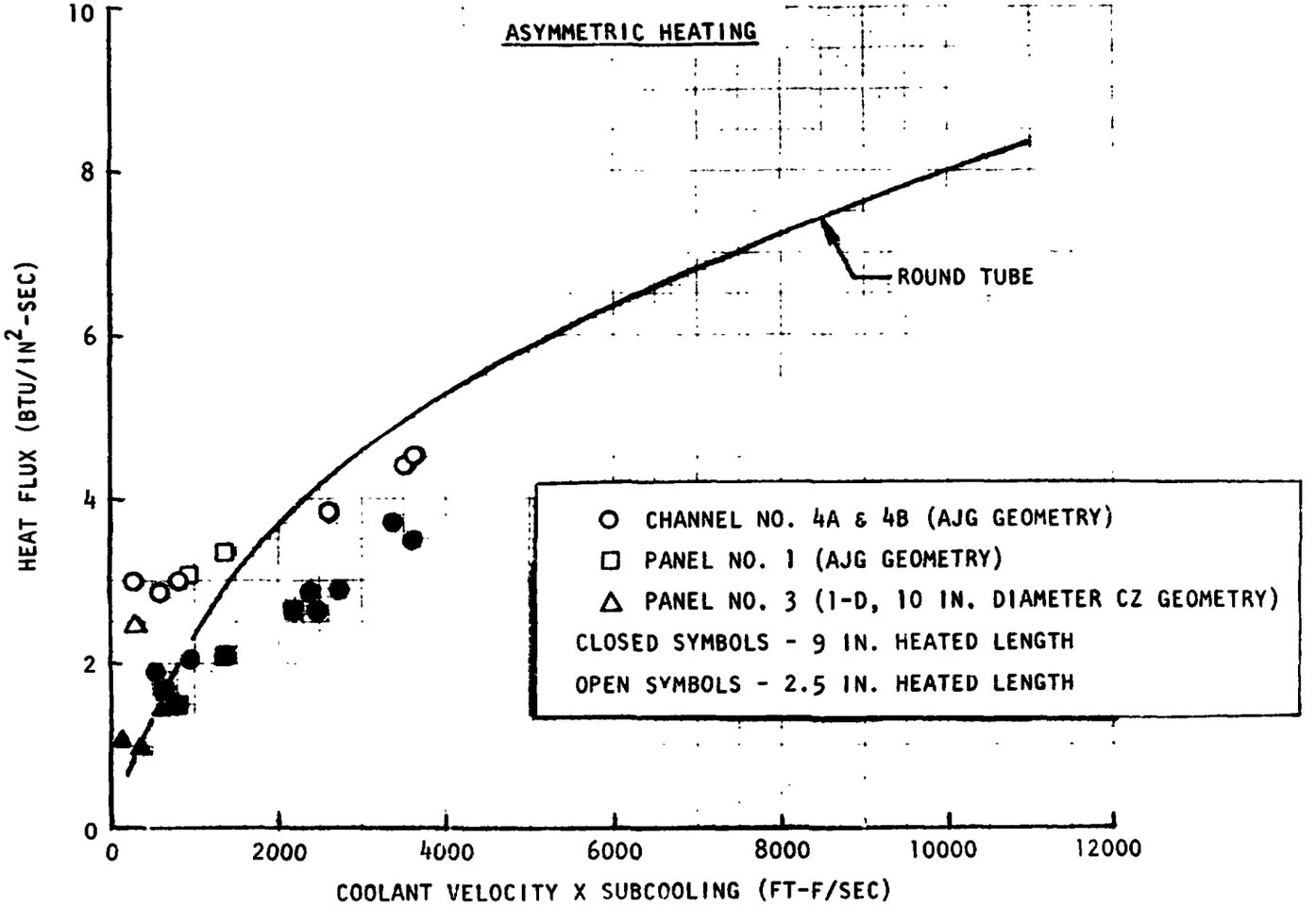

Figure 16. Comparison of Channel and Panel MMH Burnout Heat Flux

The single 2.5 inch Panel No. 3 test is seen to indicate a much higher heat flux capability than predicted from the 1-D correlation. Since this channel geometry is also similar to a throat design (i.e., narrow land width = 0.040 inch), the test result would indicate that current OME chambers may be over-designed in the throat region.

The initial helium bubble test series utilized a continuous helium flowrate in the center channel (i.e., infinite bubble) somewhat less than that which would occur in the chamber at nominal design jacket pressure drop. The purpose of the test was to determine the maximum heat flux level that could be sustained with an infinite bubble (in conjunction with adjacent channel MMH cooling at nominal flow) before proceeding with the discrete bubble tests. The results of this test series indicated, however, that an infinite bubble could be tolerated at heat flux levels approaching the nominal combustor design value of 2.0 Btu/in.^{2}-sec. The net effect of this initial test series was to eliminate the planned discrete helium bubble tests since no burnout would occur for the shorter duration (2 second maximum based on facility bubble trap volume) helium bubbles with adjacent channel MMH cooling.

The remainder of the panel tests were concerned with simulating plugged channel flow conditions. Two primary approaches were utilized. The majority of the tests were conducted with a small helium purge in the center channel to assure no trapped MMH liquid or vapors. A comparison of the low helium purge results with the initial test series which utilized a much higher helium flowrate indicated no difference in burnout limit. This implies that the helium contributes negligible cooling benefit as predicted from theoretical calculations. A lesser number of tests were conducted with nominal MMH flow in the center channel which was gradually reduced to zero. Both of these types of tests tend to simulate complete upstream plugging of a channel.

A single test (No. 103) was also conducted which simulated complete downstream plugging with MMH trapped in the test section. The center and outer flow circuits were coupled upstream of the test section to simulate effects of a common inlet manifold as utilized in OME chamber designs.

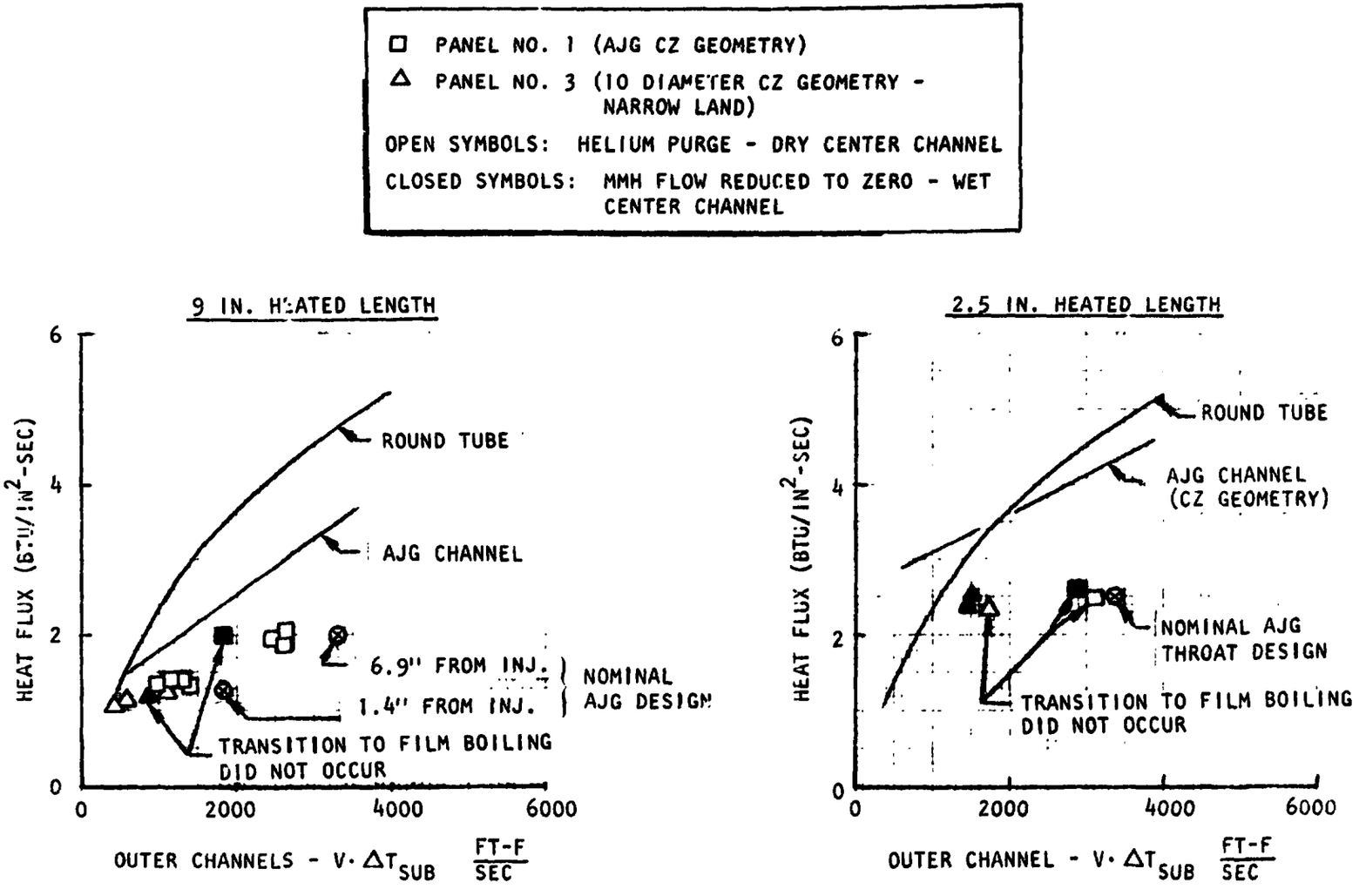

Figure 17. Effect of Completely Plugged Channel on Adjacent Channels Maximum Heat Flux Capability

Evaluation of the plugged channel tests are somewhat more difficult than simple burnout type tests. The approach taken herein was to determine the $V \cdot \Delta T_{SUB}$ parameter of the MMH flow in the outer channels when transition to film boiling occurred in the test section. This approach allows a somewhat quantitative evaluation of test results which can be applied to a chamber design to estimate safety margin with a completely plugged channel.

Not all tests underwent transition to film boiling. Testing was conducted only at nominal heat flux levels corresponding to OME throat and combustor design conditions. Hindsight indicates that, perhaps, higher heat flux levels (or reduced $V \cdot \Delta T_{SUB}$ values) should have been attempted in order to obtain a greater amount of burnout data with plugged channel operation.

The results of the plugged channel tests are compared with the nominal channel burn-out results in Fig. 17. It is apparent that there is a degradation in maximum heat flux capability with plugged channel operation. This is to be expected since the heat input to the uncooled center channel tends to concentrate in the adjacent corners of the MMH cooled channels resulting in a locally higher effective heat flux level.

Also included in Fig. 17 are the nominal AJG OME design values at various chamber locations. It should be noted that the plugged channel data indicate feasible operation at $V \cdot \Delta T_{SUB}$ values less than nominal OME design conditions. In actual practice, however, the $V \cdot \Delta T_{SUB}$ value in the channels immediately adjacent to a plugged channel will decrease due to an increased heat load with resultant decreased local subcooling. The actual extent of the reduction in $V \cdot \Delta T_{SUB}$ would require analysis of the heat transfer from the MMH in these channels to the cooler adjacent MMH cooled channels. Such an analysis was not attempted in this task.

A comparison of the data from tests 99 (upstream plugging) and 103 (downstream plugging) indicates no significant difference in the burnout correlation for these two conditions. No indication of detonation was observed during the test with the downstream plug indicating that the MMH was simply boiled out of the center channel.

In summary, the data of Fig. 17 can be utilized in conjunction with a detailed conduction analysis to estimate the reduced safety factor profile resulting from a completely plugged channel.

CONCLUSIONS

The initial test series with a symmetrically heated round CRES tube in the relocated test facility indicated excellent reproducibility of previous MMH burnout data. Helium ingestion tests in the same tube test section indicated a significant reduction in MMH burnout capability of about 15 to 20 percent. Small amounts of helium ingestion (≈ 5 percent by volume) appeared to be nearly as detrimental as the larger ingestion flowrates (≈ 20-30 percent) tested.

Asymmetrically heated single channel burnout tests simulating combustor conditions exhibited a marked reduction in the MMH burn-out heat flux capability compared to the round tube data. This reduction in apparent heat flux capability is due to heat concentration in the corners of the channel. Adequate analytical prediction of this effect appears feasible using a 2-D computer conduction model in conjunction with the 1-D correlation obtained from round tube data.

The 2-D conduction effect appears much less severe in the short channel test sections simulating throat cooling conditions (but not geometry). This result may be due to the greater subcooling associated with the short heated length. Further analytical effort is required to better understand the short test section results.

Helium ingestion tests with the single channel test sections indicated negligible effect on burn-out heat flux capabilities. It is not clear whether the reduced effect of helium ingestion on channels compared to tubes is due to geometry or asymmetric heating. Suffice to say that helium ingestion does not appear to be a problem in current OME channel design thrust chambers.

The asymmetrically heated 3-channel panel tests agreed quite well with single channel tests in regard to burnout heat flux capability. The single channel models are, therefore, a valid means of determining basic 2-D burnout data.

The infinite helium bubble and plugged channel tests indicate significant cooling is achieved by the adjacent MMH cooled channels. Testing showed that nominal heat flux levels could be sustained with zero center channel flow at V· ΔT_{SUB} values in the adjacent channels less than nominal OME design values. Actual feasibility of chamber operation with a completely plugged channel requires a detailed conduction analysis (including several channels) to determine the coolant temperature profile (and subcooling) in the channel immediately adjacent to the plugged channel. No difference was noted between upstream and downstream plugging tests.